Drug Development and Industrial Pharmacy, 2010; 36(10): 1139–1148

informa
healthcare

ORIGINAL ARTICLE

Fatty acid based hyperbranched polymeric nanoparticles for hydrophobic drug delivery

Esra Güç[1], Güngör Gündüz[2] and Ufuk Gündüz[1]

[1]*Department of Biology, Middle East Technical University, Ankara, Turkey and* [2]*Orta Doğu Teknik Üniversitesi, Kimya Mühendisliği Bölümü, Ankara, Turkey*

Abstract

Background: In recent years nano-sized dendrimer/hyperbranched polymers gained importance in drug delivery applications. *Objective*: In this study, a novel fatty acid-based hyperbranched resin (HBR) was synthesized and used for tamoxifen (TAM) and idarubicin (IDA) delivery. *Methods*: The core of the HBR was dipentaerythritol, and the branching was provided by dimethylolpropionic acid. The molecule was terminated by ricinoleic acid. Chemical and structural characterization of the resin was carried out and then drug-loading experiments were performed. *Conclusion*: The loading efficiencies were found to be 73.3% for TAM and 74% for IDA. The Fourier transform infrared spectroscopy analysis showed that TAM physically bounded onto the resin whereas IDA interacted chemically. Controlled release in phosphate buffer was improved by *Pseudomonas* sp. lipase and sodium dodecyl sulfate. The release rates decreased with the increase of loading concentrations. The cytotoxicity analyses were carried out on MCF-7 breast cancer cells for both drug-free and drug-loaded HBR. Drug-free particles did not have significant toxicity. Drug-loaded nanoparticles caused higher levels of cell death than pure drugs.

Key words: *Controlled drug delivery; hyperbranched polymer; idarubicin; nanoparticle; tamoxifen*

Introduction

Controlled drug delivery systems are designed for prolonged and effective chemotherapy. In addition, it minimizes the side effects like tissue damage and helps to eliminate the problems of early breakdown or poor solubility of drug. Various types of carriers were investigated in the past to increase the efficiency of drug delivery. Nanosized particles have been found to be highly advantageous because of the ease of circulation and penetration ability through size-dependent barriers in the body[1,2].

Dendritic or highly branched nanosized polymers are highly preferred in recent years in drug delivery. Physical and chemical properties of these nanoparticles can be easily controlled. Moreover, these polymers have many branches and/or functional end groups, which can be used for entrapping more than one type of drug, targeting agent, or solubilizer. By the incorporation of hydrophobic/hydrophilic groups, the polymer can gain lyophilic/amphiphilic properties which serve as an ideal carrier for poorly soluble drugs[3].

Hyperbranched polymers have nonsymmetrical polydispersed structures and they could be synthesized and purified by less-expensive methods with high yields[4]. One-step condensation polymerization is one of the methods to synthesize these polymers. In general, AB_x types of monomers are attached to a core molecule, and polymerization is usually carried out in the presence of a catalyst[5].

Fatty acid-based drug carriers are expected to depict least toxicity, and they are mostly preferred for hydrophobic drug delivery. These carriers have low viscosity, low melting point, and relatively high flexibility. Therefore they can be easily used for implantation and injection delivery[6]. Ricinoleic acid is a type of fatty acid that is found in castor oil at high percentage (85–90%). Its double bond is at the ninth carbon, and it has a hydroxyl group at the 12th carbon. It is the only commercially available fatty acid with two functional groups, one is acid and the other is alcohol[7].

In this study, hyperbranched resin (HBR) was synthesized using dipentaerythritol, dimethylolpropionic acid, and ricinoleic acid. The hydroxyl group of ricinoleic acid

Address for correspondence: Dr. Ufuk Gündüz, Department of Biology, Middle East Technical University, Ankara 06531, Turkey. E-mail: ufukg@metu.edu.tr

(Received 19 Jun 2009; accepted 9 Feb 2010)

ISSN 0363-9045 print/ISSN 1520-5762 online © Informa UK, Ltd.
DOI: 10.3109/03639041003691906

can make hydrogen bonding with drug molecule providing prolonged control of delivery. Idarubicin (IDA) is an anthracycline agent that is more lipophilic than its analogue daunorubicin and doxorubicin. Although IDA has less cardiotoxicity, it leads serious side effects like myelosuppression, neutropenia, cardiomyopathy, nausea, and induction of secondary tumors[8]. Tamoxifen (TAM) is a selective estrogen receptor modulator and is widely used in all stages of breast cancer therapies. However, this drug can also lead serious side effects and, most importantly, it may initiate endometrial cancer, deep vein thrombosis, pulmonary embolism, alteration in liver enzyme levels, and so on[9]. In addition, cancer cells develop resistance against TAM. Both TAM and IDA are well-known chemotherapeutic agents effective in breast cancer therapy. Encapsulating the drug in polymeric particles or attaching it on nanoparticles may provide better transport of the drug to tumor site, and controlled release can minimize the side effects and also prevent the development of resistance. Their in vitro controlled release behavior was studied in the presence of lipase from *Pseudomonas* species and sodium dodecyl sulfate (SDS). The toxicity of drug-loaded and drug-free HBR nanoparticles was tested on breast cancer cell lines (MCF-7), and their cytotoxicities were compared with that of free drug.

Materials and methods

Materials

Castor oil was donated by Akzo Nobel Kemipol (Izmir, Turkey). *p*-Toluenesulfonic acid (*p*-TSA), methanol, acetonitrile, *o*-phosphoric acid, and triethylene amine were purchased from Merck A.G. (Darmstadt, Germany); and sulfuric acid, TAM, phosphate-buffered saline (PBS) tablets, *N*,*N*-dimethylformamide (DMF), and Type XIII lipase from *Pseudomonas sp*. species from Sigma-Aldrich (St. Louis, MO, USA). Dimethylol propionic acid (DMPA) and dipentaerythritol were donated by Perstorp AB (Sweden). Trypsin–ethylene diamine tetra acetic acid (EDTA) solution (0.25% trypsin and EDTA) and cell proliferation kit (XTT-based colorimetric assay) were obtained from Biological Industries (Kibbutz Beit Haemek, Israel); RPMI 1640 medium fetal bovine serum was from Biochrom Ag. (Berlin, Germany); dialysis membranes (MwCo 3500, diameter 26 mm) were obtained from Serva (Heidelberg, Germany); magnesium sulfate heptahydrate ($MgSO_4{\cdot}7H_2O$), dimethylsulfoxide (cell culture grade), and SDS (molecular biology grade) were from Applichem (Darmstadt, Germany). MCF-7 monolayer-type human epithelial breast adenocarcinoma cell line was provided from Foot and Mouth Disease Institute (Ankara, Turkey). IDA HCl was from Pharmacia (Milan, Italy).

Characterization

Fourier transform infrared spectroscopy

Fourier transform infrared spectroscopy (FTIR) characterization of the synthesized molecules was performed by using Bruker IFS 66/S, FRA 106/S. Solid samples were pelleted with KBr (300 mg for 1 mg of sample).

Gel permeation chromatography

Molecular weight determination was performed by using gel permeation chromatography (GPC) PL-GPC 220. Samples (0.050 g) were dissolved in tetrahydrofuran (THF) and chromatography was conducted at room temperature.

Nuclear magnetic resonance

To study the structural arrangement and composition of HBR, Bruker AVANCE 300 MHz (~7 Tesla) spectrometer was used. Purified HBR (30–40 mg) samples were suspended in deuterated dimethyl sulfoxide (DMSO) and used for measurements.

Zeta potential and particle size distribution

Zeta potential and particle size were measured to determine the charge and stability of drug-loaded and drug-free HBR samples in aqueous solution. Malvern Nano-ZS zeta potential and particles size analyzer were used. Water was used as dispersant and the zeta potential values of samples were measured at 24°C.

High-performance liquid chromatography

The loaded and released drug concentrations were determined by high-performance liquid chromatography (HPLC) (Varian Prostar, Palo Alto, CA, USA). For TAM detection, Microsorb MV C18 (4.6 × 250 mm, 5 mm) column was used. Methanol:distilled water:triethylene amine mixture (93:7:0.01) was the mobile phase at a flow rate of 1 mL/min. Fluorescent detection of TAM was done at emission and excitation wavelengths of 375 and 260 nm, respectively[10]. The same column was used for the detection of released IDA, and a mixture of acetonitrile methanol, phosphoric acid, and water (3:2:1:4) was the mobile phase. The sample was injected at a flow rate of 0.8 mL/min at room temperature and the sample concentration was detected at emission and excitation wavelengths of 470 and 580 nm, respectively[11]. The liquid sample was filtered by using 0.45 μm cellulose filter before injection to HPLC column.

Synthesis of HBR

Ricinoleic acid was obtained from castor oil as described elsewhere[12]. HBR synthesis was performed in a five-necked glass reactor under reflux. The reactor was mechanically stirred and heated by using an oil

bath. Water was removed by azeotrophic distillation using toluene. In first-generation reaction (HBP-G_1), dipentaerythritol was used as core molecule and DMPA was used as branching unit. The reaction was carried out in the presence of catalyst *p*-TSA acid (0.4%, w/w) at 140°C for 3–4 hours. The second-generation reaction (HBP-G_2) was carried out by adding stoichiometric ratio of DMPA to HBP-G_1.

Finally, HBP-G_2 was esterified by castor oil fatty acids at 220°C. The reaction was stopped when the acid number was below 40. The castor oil contains 85% ricinoleic acid and 15% other acids (linoleic acid 3%, oleic acid 7%, stearic acid 1%, and palmitic acid 2%). It was believed that the different conformations of other fatty acids with cis-type double bonds at different carbon atoms could improve the attachment of drugs on resin. Stearic acid is trans-acid and has high melting point of 70°C. It was removed by centrifugation at 21,000 × *g* for 15 minutes at 15°C (Thermo IEC, Micromax RF, Freehold, NJ, USA). To remove small molecules, the synthesized polymer was washed with pure methanol. The proposed nanostructure of HBR is given in Figure 1.

Loading of TAM and IDA on HBR nanoparticles

TAM and IDA were dissolved in DMF and were directly added to HBR. Samples were shaken at 300 rpm overnight. Then methanol was added to the mixture to dissolve unloaded drug molecules, and the mixture was centrifuged at 21,000 × *g* for 30 minutes at room temperature. The drug-loaded HBR pellets were first dried and then dissolved in DMF. The loading efficiency of IDA was analyzed by using UV–Vis spectrophotometer (Schimadzu UV-1208, Kyoto, Japan) at 540 nm, whereas TAM-loading efficiency was detected by using HPLC. The experiments were performed at dark because of light sensitivity of TAM. Loading efficiency was determined from the following formula:

$$\text{Loading efficiency (\%)} = \frac{\text{Weight of drug loaded (mg)}}{\text{Initial weight of drug (mg)}} \times 100 \quad (1)$$

Controlled drug release studies

In vitro release was performed by dialysis in screw-capped vials using 3 mL of 0.01 M PBS (pH 7.4) as release medium containing 0.5% (w/v) of SDS and 2% of lipase form *Pseudomonas* sp. (4 mg/mL). SDS prevents adsorption of TAM to the surface of test tubes and dialysis membranes, and also it improves the solubility of the hydrophobic drug[13,14]. IDA is poorly soluble in water; therefore, SDS was added to the medium. In addition, *Pseudomonas* sp. lipase was added to increase the degradation of HBR to improve drug release rate. At certain time intervals, the medium outside the dialysis membrane was removed from the vial and fresh medium was added. The samples were analyzed by HPLC and cumulative release profiles were determined.

Cell culture

MCF-7 cell cultures were maintained in RPMI 1640 medium with 10% fetal bovine serum and 1% gentamicin. Subculturing of cells was carried out by trypsinization and by diluting cells with fresh medium. Cells were incubated in the presence of 5% CO_2 at 37°C.

Cell proliferation assay

Cell proliferation assay was performed in 96-well plates. HBR nanoparticles were dissolved in dimethyl sulfoxide and then 100-fold dilution was made by using RPMI 1640 medium. About 5000 cells were seeded per well and incubated in humidified CO_2 incubator at 37°C for periods of 72 and 96 hours. By the end of incubation, XTT and activator reagents were added. After incubation in dark for 2–5 hours, the intensity of the color was measured by using ELISA reader (SPECTRAmax 340PC, San Diego, CA, USA) at 500 nm. Half maximal inhibitory concentration (IC_{50}) value of the samples was determined by using logarithmic viability curves.

Statistical analysis

Minitab Statistical Software (Minitab Inc., State College, PA, USA) was used to determine the significant differences between the mean of the groups ($\alpha = 0.05$). Two-sample *t*-test was used for statistical analysis.

Results and discussion

Characterization of HBR nanoparticles

FTIR spectroscopy

The FTIR spectrum of HBR before and after ricinoleic acid esterifications is shown in Figure 2.

The IR spectrum of pure ricinoleic acid was also determined for comparison (data not shown). The small peak at 3015 cm^{-1} corresponded to olefinic C-H stretch of fatty acids and it was not observed in HBP-G_2. The frequency at 1735 cm^{-1} corresponds to ester functional groups; 1464 cm^{-1} corresponds to methylene C-H bend; and the peak at 1245 cm^{-1} belongs to O=C-O-C stretching of aliphatic polyesters. The peak at 725 cm^{-1} is due to rocking of methylene groups of ($n \geq 3$) of fatty acids in HBR.

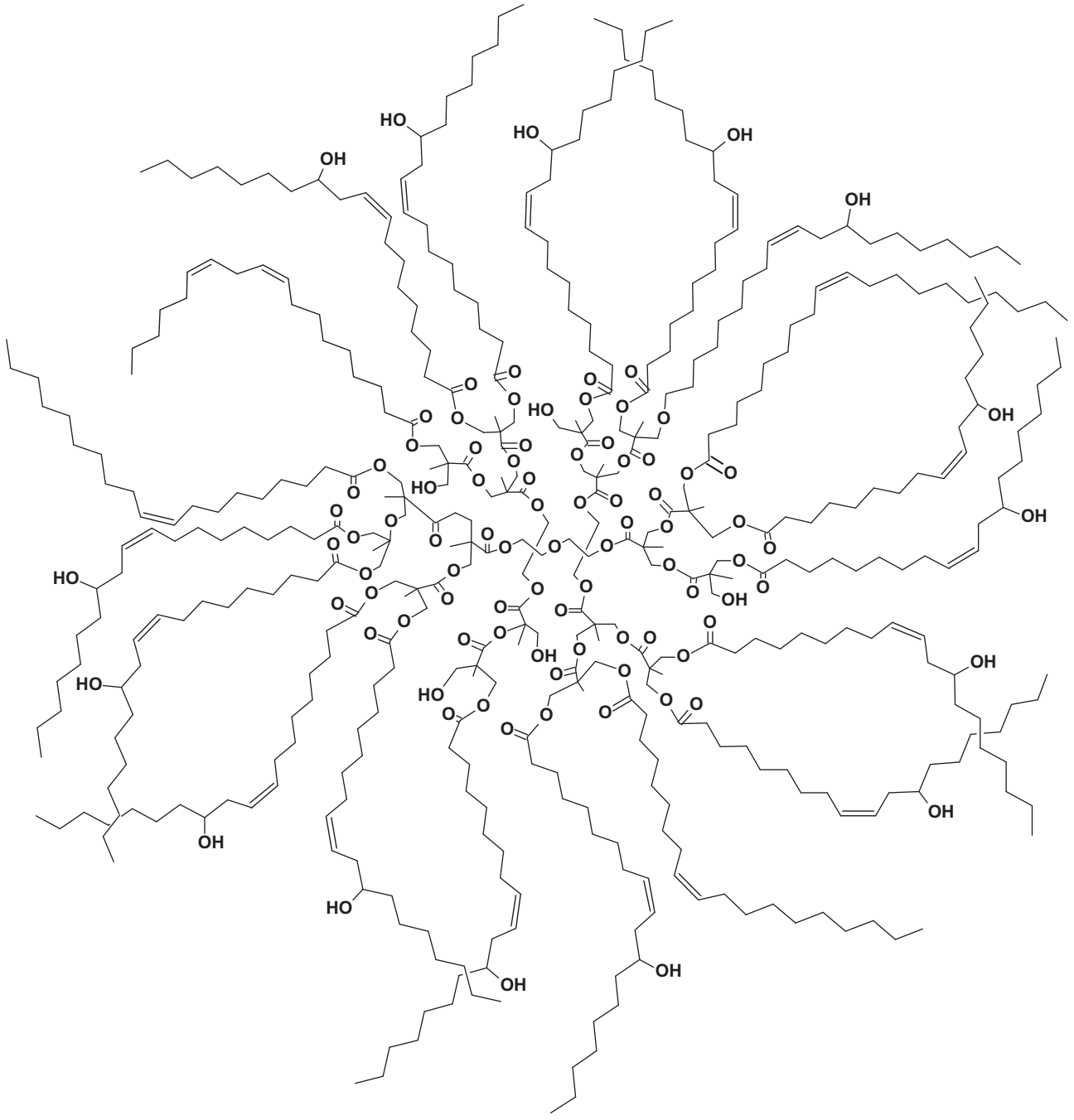

Figure 1. Representative structure of HBR.

Liquid ^{13}C NMR analysis of HBR

To confirm the characteristic carbon atoms of HBR, 13C nuclear magnetic resonance (NMR) was performed. Figure 3a shows the carbon atoms of one of the branches of HBR. The numbers indicate the carbon atoms.

The 69.73 ppm peak in Figure 3b corresponds to carbon atom involved in ether bond of dipentaerythritol (i.e., #1 in Figure 3a); 174.56 ppm to carbon atom involved in ester bond (i.e., #2 in Figure 3a). The 31.34 ppm corresponds to #3, 26.68 ppm to #4, and 24.73 ppm to #5. In the same way, 40.27 ppm corresponds to #6, 48.55 ppm to #7, 130.00 ppm to #8, 124.44 ppm to #9, 40.00 ppm to #10, 38.61 ppm to #11, and 14.1 ppm to #12 on the ricinoleic branch.

Molecular weight determination

The determination of molecular weight was accomplished by GPC. The molecular weight was determined

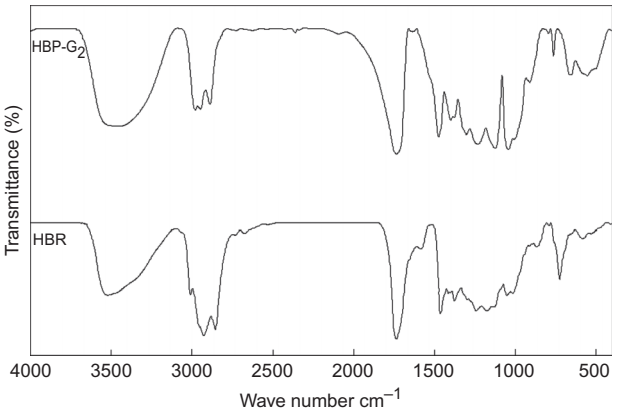

Figure 2. FTIR spectra of HBR and HBP-G_2.

after the purification of HBR with methanol. The weight average molecular weight (M_w) of HBR was determined to be 23,100 ± 3000 g/mol, and the number average molecular weight (M_n) was determined to be 10,900 ± 90 with a polydispersity of 2.11. Because HBR nanoparticles were synthesized by condensation polymerization at the appropriate molar ratios, polydispersity value was in expected range, which was close to 2.

TAM- and IDA-loading efficiencies

The loading efficiencies of TAM and IDA are given Figure 4a and b, respectively.

The maximum loading efficiency of TAM was achieved as 73.3% at 0.7 µg/mg as seen in Figure 4a. The

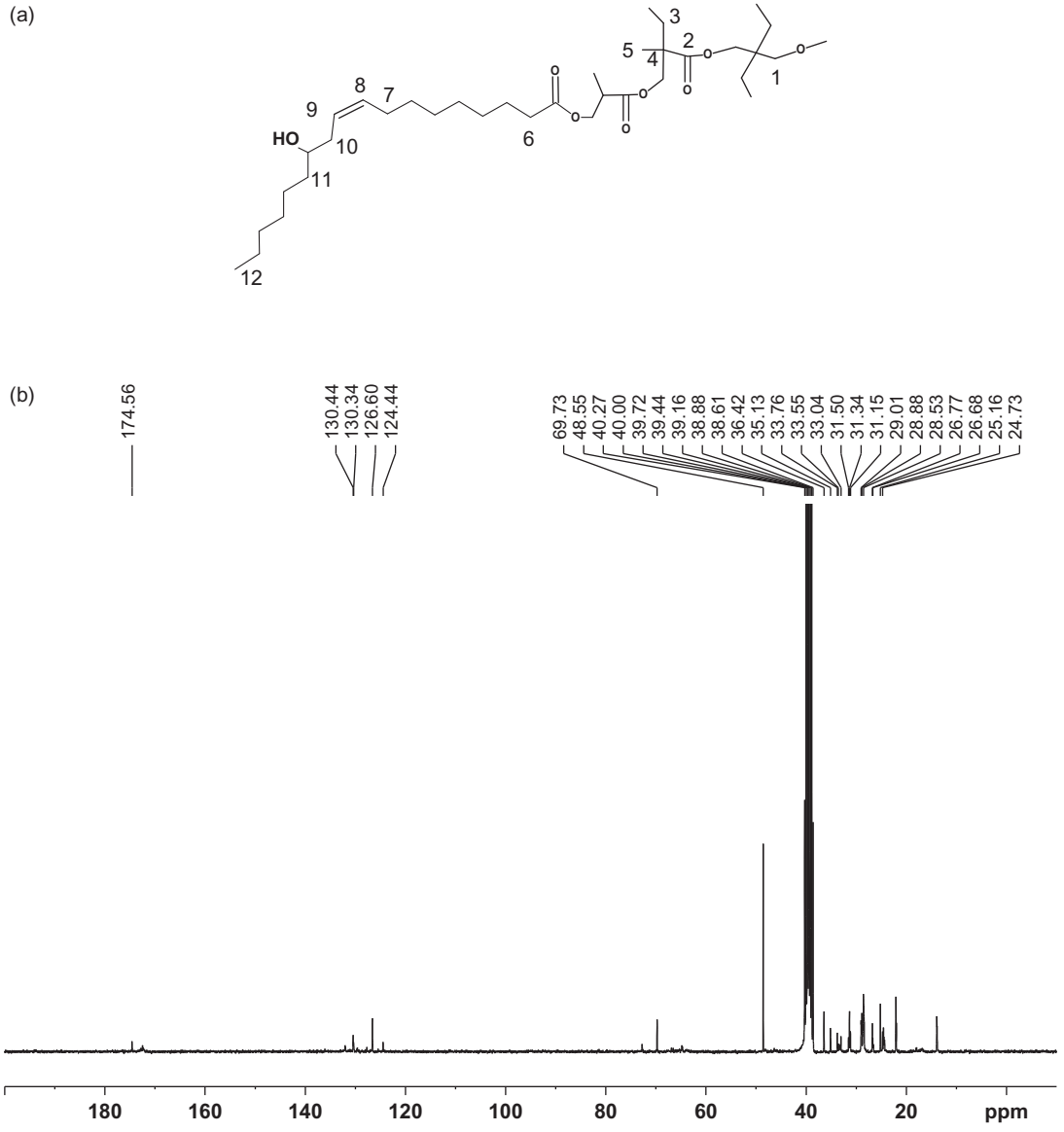

Figure 3. (a) One of the branches of HBR; (b)^{13}C NMR of HBR.

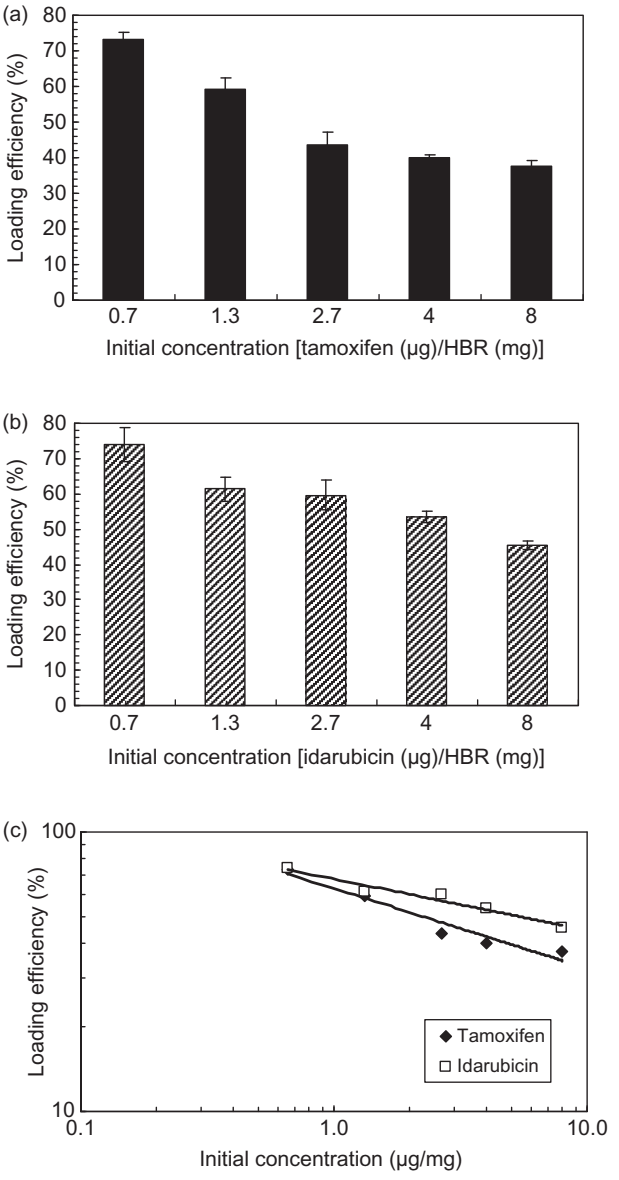

Figure 4. (a) Loading efficiency of tamoxifen; (b) loading efficiency of idarubicin; (c) loading efficiency on log–log scale.

highest efficiency for IDA was found to be 74% for the concentration of 0.7 μg/mg, and the lowest efficiency was 45.3% for 8 μg/mg (Figure 4b). The increase in the drug concentration leads to a decrease in loading efficiency. The change is particularly pronounced for TAM.

Although IDA and TAM entrapment efficiencies were different, they exhibited similar decline behavior. The encapsulation profile of resin for both drugs was plotted on log–log scale in Figure 4c. The semilog plot [i.e., log (efficiency) versus initial concentration] did not give a straight line, that means, the attachment of drug molecules on nanoparticles is not a random process. Figure 4c indicates that the change obeys a power law behavior, such that,

$$\text{for tamoxifen,} \quad \text{loading efficiency} = 62.8\,C^{-0.286} \tag{2}$$

$$\text{for idarubicin,} \quad \text{loading efficiency} = 67.9\,C^{-0.184} \tag{3}$$

where 'C' denotes the initial concentration of drug. These relations can be easily obtained from log–log plots. The slope of the line obtained from log–log plot gives the scaling power. It is seen that TAM with a scaling power of '−0.286' is detached from resin much faster than IDA, which has a scaling power of '−0.184.'

Chemical characterization of drug-loaded HBR

The IR spectra of drug-free HBR, TAM-loaded HBR (HBR-TAM), and IDA-loaded HBR (HBR-IDA) are shown in Figure 5.

After TAM loading, no change in IR spectrum was observed compared to drug-free HBR, which indicates no chemical interaction between TAM and the polymer. Moreover, chemical groups of TAM were not identified because the concentration of drug was quite low. The chemical groups of the drug might be masked by chemical groups of HBR. Similar results were obtained in the literature[15,16]. TAM bound on HBR could be detected by HPLC analysis. On the contrary, chemical interaction was seen between IDA and HBR because a new peak at 1675 cm^{-1} was displayed in Figure 5. It does not exist either in FTIR spectrum of pure IDA (data not shown) or in drug-free HBR. A detailed spectrum analysis must be carried out to identify the type of chemical interaction.

As mentioned before, the increase of the concentration of drug results in a decrease of entrapment efficiency. The decrease of efficiency depicts a power law

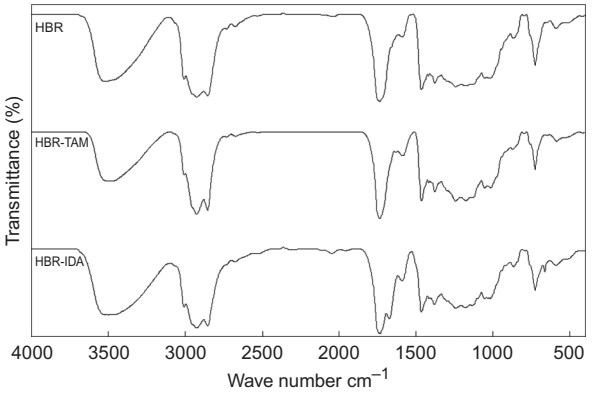

Figure 5. FTIR spectra of HBR, HBR-TAM, and HBR-IDA.

behavior for both drugs as given by Equations (2) and (3). IDA has a lower scaling power than TAM and this difference can be well understood from the FTIR analysis. The chemical interaction of IDA naturally lowers its rate of detachment from HBR.

Particle size distribution and zeta potential

Particle size distribution plays an important role in drug release. Reports indicate that small particles (<500 nm) could pass through epithelial barriers by endocytosis, which sustains an advantage for nanoparticles to permeate across physiological drug barriers[17,18]. The particle size of HBR, HBR-TAM, and HBR-IDA are given in Table 1.

Two different initial drug concentrations (2.7 and 8 μg/mg) were used in drug-loading experiments. The third column in Table 1 shows the determined loading efficiencies corresponding to these initial drug concentrations. The particle size varied between 206.9 and 276.5 nm as seen from the fourth column of the table. The particle size analysis was carried out by introducing a drop of HBR dissolved in DMF into water cuvette. It seems that HBR molecules aggregated because of hydrophobic interaction in aqueous medium.

Table 1 shows that after TAM and IDA loading the particle sizes get smaller. Strong hydrophobic interaction between the drug and the polymer results in a decrease of average particle size in aqueous solutions. After drugs are entrapped onto HBR, the fatty acid residues may wrap around the drug causing a kind of reduction in size. It is also possible that the drugs added on HBR may decrease the aggregation of HBR molecules by restricting the hydrophobic interaction of ricinoleic acid residues. In the study of Maillard et al.[19] and Chu et al.[20], this type of observation was explained by low solubility and compact structure of the carrier and hydrophobicity of drugs.

Table 1 also displays zeta potentials of the nanoparticles. Particles with zeta potential between −30 and +30 mV have physical instability in aqueous solutions[21]. In our case, the potential values changed between −40.2 and −43.7 mV, which indicated that the nanoparticles are stable. Duerr-Auster et al. studied the zeta potential of polyglycerol esters of fatty acids and found out that the zeta potential was almost −40 mV around a pH of 7, and they also reported that it decreases as the pH increases. The HBR synthesized in our study has similar functional groups and a similar zeta potential was obtained at pH of 6.8.

The zeta potential of drug-free HBR nanoparticles did not significantly change after drug loading even at high drug concentrations. As the drug/polymer ratio is low, the entrapped drug might not show an effect on zeta potential[22,23].

In vitro drug release

In preliminary studies, the release of TAM was investigated in PBS buffer; however, very small amount of drug was released even after 100 days. Our previous studies from the measurement of the molecular weight changes in PBS-suspended lipase indicated the molecular degradation of HBR compared to the lipase-free buffer at pH 7.4. To improve the release, 0.5% (w/v) SDS and 2% (v/v) lipase were added to the medium[13,14]. Lipase from *Pseudomonas* sp. is known to be effective in creating surface erosion and degrading various polymeric structures[24].

The samples had initial concentrations of 2.7 and 8 μg/mg TAM. For the initial loading concentration of 2.7 μg/mg, the release effectively began after the fifth day, and 93% of the loaded drug was released in 25 days. The release was linear until 25th day, and no significant release was observed by the end of 55th day (Figure 6a).

When the initial loading of TAM was increased to 8 μg/mg, a linear change with respect to time was observed until 12th day with 42% release. Then it slowed down and followed another linear path with a final total release of 58% by the end of 25th day. Again, no significant release was observed afterwards. As observed, the increase of the initial loading of the drug caused a decrease in the release rate. This may be due to the fact that the drug molecules aggregate at certain sites on HBR nanoparticles because of their hydrophobicity. Therefore, the surface area decreases per unit weight of drug. This may naturally decrease the rate of drug release that takes place on the surface. The release profile of IDA is given in Figure 7a.

As it is seen from Figure 7, less than 1% release was observed in 75 days in 0.01 M PBS buffer (pH 7.4, 0.5% SDS, 2% lipase at 37°C) for initial concentrations of both 2.7 and 8 μg/mg. The FTIR spectrum depicted a kind of

Table 1. Some characteristics of HBR, HBR-TAM, and HBR-IDA.

Samples	Initial drug concentration (μg/mg)	Loading efficiency (%)	Particle size (nm)	PDI	Zeta potential (mV)
HBR	—	—	276.5 ± 8.6	0.187 ± 0.005	–41.2 ± 0.7
HBR-TAM	2.7	40 ± 1.4	232.2 ± 2.7	0.172 ± 0.002	−43.7 ± 2.2
	8	37.5 ± 1.7	206.9 ± 0.01	0.142 ± 0.012	−40.2 ± 1.2
HBR-IDA	2.7	59.6 ± 4.3	217.1 ± 5.6	0.156 ± 0.014	−41.4 ± 1.6
	8	45.3 ± 1.2	215.2 ± 4.2	0.163 ± 0.003	−40.6 ± 0.1

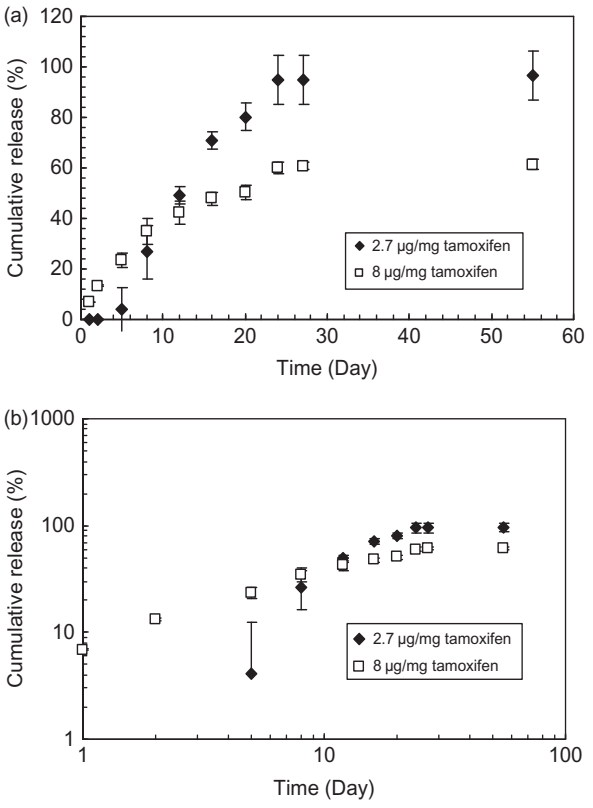

Figure 6. (a) Cumulative release of tamoxifen; (b) cumulative release of tamoxifen on log–log scale.

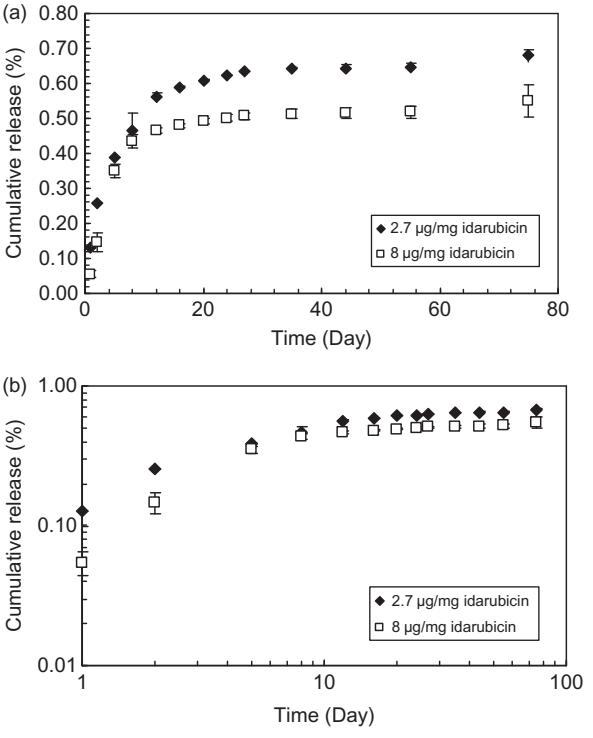

Figure 7. (a) Cumulative release of idarubicin; (b) cumulative release of idarubicin on log–log scale.

chemical interaction of IDA with HBR polymer as seen from Figure 5; thus slow release was expected for this drug. Slow IDA release may also be explained by unsuitable release medium. SDS was added to increase the solubility of IDA and TAM. Although TAM release was improved by SDS addition, it seems that the IDA release could not be improved. On the contrary, when HBR-IDA was applied on MCF-7 cells, drug toxicity was good indicating that release of the drug in cell culture conditions was much better than in dialysis release experiments (Section under *Cytotoxicity of drug-free and drug-loaded HBR*). TAM and IDA release rate and their efficiencies could be improved by using higher enzyme concentrations and varying pH conditions.

It should be noted that enzymatic degradation profiles that are performed in buffer should not be correlated with in vitro cell culture and in vivo experiments. After cellular uptake, lysosome–endosome enzyme activities affect the degradation. In addition, acidic pH in both phagosomes and endosomes could change the drug release and polymer degradation profiles[25,26].

To understand the dynamics of drug release, the cumulative release versus time was plotted on log–log scale; Figure 6b is for TAM and Figure 7b is for IDA. It is seen from Figure 6b that the release rate for 8 µg/mg case follows a straight line, so there is only one release dynamics for this concentration of TAM. In the case of 2.7 µg/mg initial concentration, the release curve is not a straight line. Therefore, the release dynamics at this low concentration seems to be highly complex. At high initial concentration of loading, it is possible that multilayer attachments occur on HBR, and the amount of detached drug correlates with the amount attached. That is, if a drug molecule is released it pulls out the molecules below causing a kind of block desorption. At low initial concentrations of loading, the drug can attach on different regions of HBR without forming multilayers. Thus the detachment occurs because of the breaking of weak chemical bonds between the drug and the polymer. Once some of the drug molecules are released, the fatty acid residues may become free and change their configuration by affecting the detachment mechanism of the remaining drug molecules. Further investigations needs to be done to reveal the actual mechanism of drug detachment at low and high loading concentrations.

In the case of IDA, there are two different release dynamics as seen from Figure 7b for both low and high loading concentrations. A fast release between 8 and 10 days is followed by a slow release rate thereafter for both concentrations. In the fast release regime, it is possible that the hydrophobically aggregated drug molecules break up and leave the HBR. The remaining attached drug molecules need much longer time to break up their bonds with polymer resin.

Cytotoxicity of drug-free and drug-loaded HBR

Figure 8 shows cell viability of MCF-7 cells after 96 hours of incubation with HBR.

The concentration of HBR was changed between 1.59 and 812 μg/mL. The toxicity profile of drug-free HBR indicated that 812 and 406 μg/mL concentrations caused a mild level toxicity. The lowest cell viability determined for 812 μg/mL of HBR treatment was 52.6%. These results indicated that exposing drug-free HBR even after 96 hours of incubation was well tolerated by cells. Figure 8 also shows cytotoxicity profiles after HBR-IDA and HBR-TAM treatments. HBR-TAM and HBR-IDA concentrations between 25.4 and 812 μg/mL displayed a significant toxicity relative to drug-free HBR. The cell proliferation at the highest HBR-IDA (812 μg/mL) was determined as 27.5%.

Table 2 shows the comparison of half maximal inhibitory concentration values of drug-loaded HBR samples with those of pure TAM and pure IDA after 72 and 96 hours of incubations.

The amount of pure drugs was taken to be equal to loaded drugs. HBR-TAM exhibited 12.8- and 5-fold more toxicity relative to pure TAM at the incubation times of 72 and 96 hours, respectively. Moreover, HBR-IDA after 72 and 96 hours of incubation displayed 2.1- and 1.5-fold toxicity compared to pure IDA.

Dialysis-based release displayed a slower drug release profile; however, cytotoxicity profiles showed the high potency of drug-loaded HBR formulations on breast cancer cells. Ulbrich et al.[25] suggested that nanoparticles were taken up by endosomes and could release their drug by pH-controlled hydrolysis or specific enzymatic degradation in lysosomes. As the diameter of HBR-IDA and HBR-TAM were suitable for endosomal uptake, the drug release might be speeded up by the aid of endosomes and lysosomes. Therefore, under favorable cell metabolism conditions, the release could be faster and the effect of HBR nanoparticles could be observed in shorter periods of time compared to in vitro release systems.

It has been known that drug uptake by MCF-7 cells occurs through passive diffusion, and drug molecules can be effluxed from the cells by P-gp pumps[27]. The function of these pumps is to protect cells from toxic effects of some chemicals. However, in case of chemotherapy, this leads to drug-resistance by lowering the drug concentration in cancer cells. After application of pure IDA or TAM to MCF-7 cells, some of the drug will probably removed out of the cell by these drug pumps. However, drug-loaded HBR particles will not be recognized by the drug efflux pumps. Multidrug resistance is one of the major problems in cancer chemotherapy, and this type of drug delivery system could be expected to overcome drug resistance. Besides, as mentioned previously, nanoparticles might enter into cells by endocytosis and drug release might start by degradation of the polymer. Thus, the time of the interaction of the drug with the cells will be longer than the free drug, which may cause a higher affectivity on cancer cells.

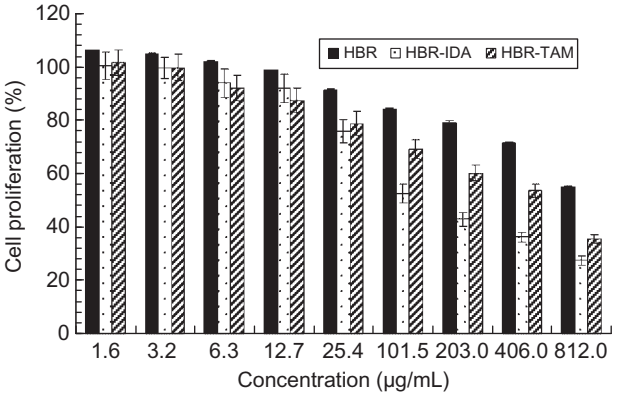

Figure 8. Cell proliferation profiles of MCF-7 cells after 96 hours of incubation.

Table 2. IC_{50} values of drug-loaded HBRs and pure drugs.

IC50 (μM)	72 hours	96 hours
HBR-TAM	3.5 ± 0.43	1.33 ± 0.02
TAM	44.8 ± 2.6	6.9 ± 0.5
HBR-IDA	2 ± 0.02	0.68 ± 0.01
IDA	4.2 ± 0.2	1 ± 0.27

Conclusion

In this work, novel type of HBR nanoparticles were used for drug delivery. TAM and IDA were loaded on nanoparticles at 73–74% efficiencies. FTIR analysis showed that TAM physically bounded on nanoparticles whereas IDA formed chemical bonds. The zeta potential of drug-loaded and drug-free HBR were around −40 mV indicating the stability of HBR in aqueous solution. The polymeric nanoparticles could be completely degraded in the presence of lipase. In the presence of lipase and SDS, the release of TAM for the initial concentration of 2.7 μg/mg of polymer was 93%, whereas at 8 μg/mg it was 58% by the end of 25th day. On the contrary, the release of IDA in the test tube was quite poor. However, when MCF-7 cells were exposed to TAM- and IDA-loaded particles, it was observed that in 48 hours cell killing increased by 109- and 4.8-fold, respectively, compared to free drugs.

Acknowledgments

This project was supported by Türkiye Bilimsel ve Teknolojik Araştırma Kurumu (TUBİTAK, 107T179). We

are grateful to Ali Uğur Ural (Professor in Gülhane Military Medical School Hospital, Department of Hematology, Ankara, Turkey) for donating IDA.

Declaration of interest

The authors report no conflicts of interest. The authors alone are responsible for the content and writing of this paper.

References

1. Brannon-Peppas L, Blanchette JO. (2004). Nanoparticle and targeted systems for cancer therapy. Adv Drug Deliv Rev, 56:1649–59.
2. Nori A, Kopecek J. (2005). Intracellular targeting of polymer-bound drugs for cancer chemotherapy. Adv Drug Deliv Rev, 57:609–36.
3. Gupta U, Agashe HB, Asthana A, Jain NK. (2006). Dendrimers: Novel polymeric nanoarchitectures for solubility enhancement. Biomacromolecules, 7:649–58.
4. Paleos CM, Tsiourvas D, Sideratou Z. (2007). Molecular engineering of dendritic polymers and their application as drug and gene delivery systems. Mol Pharm, 4:169–88.
5. Bharathi P, Moore JS. (2000). Controlled synthesis of hyperbranched polymers by slow monomer addition to core. Macromolecules, 33:3212–8.
6. Sokolsky-Papkov M, Shikanov A, Kumar N, Vaisman B, Domb AJ. (2008). Fatty acid based biodegradable polymers-synthesis and applications. Bull Israel Chem Soc, 23:12–7.
7. Jain JP, Modi S, Kumar N. (2008). Hydroxy fatty acid based polyanhydride as drug delivery system: Synthesis, characterization, in vitro degradation, drug release, and biocompatibility. J Biomed Mater Res, 84:740–52.
8. Blasiak J, Gloc E, Warszawski M. (2002). A comparison of the in vitro genotoxicity of anticancer drugs idarubicin and mitoxantrone. Acta Biochim Pol, 49(1):145–55.
9. Bhatia A, Singh B, Singh B, Bhushan S, Katare OP. (2009). Tamoxifen-encapsulated vesicular systems: Cytotoxicity evaluation in human epidermal keratinocyte cell line. Drug Dev Ind Pharm, iFirst:1–5.
10. Long BJ, Jelovac D, Handratta V, Thiantanawat A, MacPherson N, Ragaz J, et al. (2004). Therapeutic strategies using the aromatase inhibitor letrozole and tamoxifen in a breast cancer model. J Natl Cancer Inst, 96:456–65.
11. Fukushima T, Inoue H, Takemura H, Kishi S, Yamauchi T, Inai K, et al. (1998). Idarubicin and idarubicinol are less affected by topoisomerase II-related multidrug resistance than is daunorubicin. Leuk Res, 22:625–9.
12. Bat E, Gündüz G, Kısakürek D, Akhmedov IM. (2005). Synthesis and characterization of hyperbranched and air drying fatty acid based resins. Prog Org Coating, 55:330–6.
13. Chawla JS, Amiji MM. (2002). Biodegradable poly(ε-caprolactone) nanoparticles for tumor targeted delivery of tamoxifen. Int J Pharm, 249:127–38.
14. Hu FX, Neoh KG, Kang ET. (2006). Synthesis and in vitro anticancer evaluation of tamoxifen-loaded magnetite/PLLA composite nanoparticles. Biomaterials, 27:5725–33.
15. Tayade PL, Kale RD. (2004). Encapsulation of water insoluble drug by a cross-linking technique: Effect of process and formulation variables on encapsulation efficiency, particle size, and in vitro dissolution rate. AAPS Pharm Sci, 6:1–8.
16. Vishnu YV, Chandrasekhar K, Ramesh G, Rao YM. (2007). Development of mucoadhesive patches for buccal administration of carvedilol. Curr Drug Deliv, 4:27–39.
17. Dong Y, Feng SS. (2004). Methoxy poly(ethylene glycol) poly(lactide) (MPEG-PLA) nanoparticles for controlled delivery of anticancer drugs. Biomaterials, 25:2843–9.
18. Yu L, Zhang H, Cheng SX, Zhuo RX, Li H. (2006). Study on the drug release property of cholesteryl end-functionalized poly(epsilon-caprolactone) microspheres. J Biomed Mater Res B Appl Biomater, 77(1):39–46.
19. Maillard S, Ameller T, Gauduchon J, Gougelet A, Gouilleux F, Legrand P, et al. (2005). Innovative drug delivery nanosystems improve the anti-tumor activity in vitro and in vivo of antiestrogens in human breast cancer and multiple myeloma. J Steroid Biochem Mol Biol, 94:111–21.
20. Chu H, Liu N, Wang X, Jiao Z, Chen Z. (2009). Morphology and in vitro release kinetics of drug-loaded micelles based on well-defined PMPC–b–PBMA copolymer. Int J Pharm, 371:190–6.
21. Duerr-Auster N, Eisele T, Wepf R, Gunde R, Windhab EJ. (2008). Influence of pH on colloidal properties and surface activity of polyglycerol fatty acid ester vesicles. J Colloid Interface Sci, 327:446–50.
22. Ameller T, Marsaud V, Legrand P, Gref R, Barratt G, Renoir JM. (2003). Polyester–poly(ethylene glycol) nanoparticles loaded with the pure antiestrogen RU 58668: Physicochemical and opsonization properties. Pharm Res, 20:1063–70.
23. Cavallaro G, Maniscalco L, Licciardi M, Giammona G. (2004). Tamoxifen-loaded polymeric micelles: Preparation, physicochemical characterization and in vitro evaluation studies. Macromol Biosci, 4:1028–38.
24. Calil MR, Gaboardi F, Bardi MAG, Rezende ML, Rosa DS. (2007). Enzymatic degradation of poly (ε-caprolactone) and cellulose acetate blends by lipase and α–amylase. Polym Test, 26(2): 257–61.
25. Ulbrich K, Subr V. (2004). Polymeric anti-cancer drugs with pH-controlled activation. Adv Drug Deliv Rev, 56:1023–50.
26. Zhang Z, Kuijer R, Bulstra SK, Grijpma DW, Feijen J. (2006). The in vivo and n vitro degradation behavior of poly(trimethylene carbonate). Biomaterials, 27:1741–48.
27. Vaulthier C, Dubernet C, Chauvierre C, Brigger I, Couvreur P. (2003). Drug delivery to resistant tumors: The potential of poly(alkyl cyanoacrylate) nanoparticles. J Control Release, 93:151–60.